



# Hydrogeochemical characteristics, source distribution, and health risk of high-fluoride groundwater in Swabi, Pakistan

Muhammad Tariq · Abdur Rashid · Seema Anjum Khattak · Liaqat Ali · Mohammad Tahir Shah

Received: 15 February 2024 / Accepted: 26 November 2024 / Published online: 6 December 2024  
© The Author(s), under exclusive licence to Springer Nature Switzerland AG 2024

**Abstract** This paper evaluated fluoride ( $F^-$ ) pollution in drinking groundwater sources, which causes severe fluorosis and other human health concerns in Swabi, Pakistan. We determined  $F^-$  concentration, prevalence, enrichment, distribution, and health hazards from water ingestion in Swabi, Pakistan. Therefore, 126 groundwater and 18 surface water samples were collected to analyze  $F^-$  and other geochemical tracers to understand groundwater enrichment and  $F^-$  mobilization in aquatic systems. The range and mean values of  $F^-$  in groundwater were 0.02 to 14.2 and 4.0 mg/L, and those in surface water were 1.12–0.8 and 1.4 mg/L. Most residents used groundwater for drinking purposes. Thus, groundwater results showed that 72.2% of samples had surpassed the WHO guidelines of  $F^-$  1.5 mg/L. The fluoride pollution index

(FPI) declared that 48.73% of samples showed a higher risk, 41.95% medium risk, and 9.32% lower risk. Mineral phases using PHREEQC interactive software determined mineral saturation revealing the dissolution of host rock minerals and unsaturation showed precipitation of minerals within the aquifer. The principal component analysis multilinear regression (PCA-MLR) model showed a five-factor solution: (a) geogenic processes, (b) mixed geogenic and anthropogenic inputs, (c) geochemical processes, (d) agriculture pollution, and (e) industrial effluents which would release  $F^-$  in the aquifer. The health hazard due to higher  $F^-$  revealed that children showed high-risk levels compared to adults in endemic areas. The spatial distribution of  $F^-$  in drinking groundwater increases towards the northern side and decreases in the south to the southeastern side. Therefore, effective water management techniques would be required to safeguard groundwater resources and secure human

---

**Supplementary Information** The online version contains supplementary material available at <https://doi.org/10.1007/s10661-024-13458-5>.

M. Tariq · A. Rashid · S. A. Khattak · L. Ali (✉)  
M. T. Shah

National Centre of Excellence in Geology, University of Peshawar, Peshawar 25130, Pakistan  
e-mail: liaqat.nceg@uop.edu.pk

M. Tariq  
e-mail: muhammadtariq332@gmail.com

S. A. Khattak  
e-mail: s\_anjum@uop.edu.pk

M. T. Shah  
e-mail: tahir\_shah@uop.edu.pk

A. Rashid (✉)

Key Laboratory of Urban Environment and Health, Institute of Urban Environment, Chinese Academy of Sciences, Xiamen 361021, China  
e-mail: abdur.rashid@bs.qau.edu.pk

A. Rashid

State Key Laboratory of Biogeology and Environmental Geology, School of Environmental Studies, China University of Geosciences, Wuhan 430074, People's Republic of China

health from dental and skeletal fluorosis and other associated problems caused by high F<sup>-</sup> groundwater with varying fluoride concentrations. This study will help the water management authority to safeguard depleted groundwater for drinking demands.

**Keywords** Groundwater pollution · Fluoride contamination · Spatial distribution · Health risk assessment · Swabi, Pakistan

## Introduction

Water is the basic component of life on earth and encompasses different minerals, which are an important constituent of human nutrition (Cannas et al., 2020). Groundwater is commonly used for drinking, domestic, irrigation, and industrial demands (Rashid et al., 2023d, 2024a). Worldwide, groundwater pollution is a significant public health issue, impacting millions of people, especially in areas where groundwater serves as the main source of drinking water (Xie et al., 2023). Thus, natural and human-induced pollutants can compromise groundwater quality, posing serious risks to public health (Rashid et al., 2023b, 2024b). Both surface and groundwater have been widely contaminated by heavy elements (HEs) such as cadmium (Cd), chromium (Cr), lead (Pb), mercury (Hg), copper (Cu), arsenic (As), manganese (Mn), and cobalt (Co) (Rashid et al., 2019, 2021, 2023c) and anions, viz. fluoride (F<sup>-</sup>) and nitrate (NO<sub>3</sub><sup>-</sup>) (Ayub et al., 2024). The deterioration of water quality in general and the decline of groundwater are significant. Therefore, qualitative and quantitative clean water is important for the security of human generation. Contaminated groundwater is the cause of waterborne diseases, and 65% resulted from high F<sup>-</sup> groundwater (Rashid et al., 2020).

Globally, F<sup>-</sup> is a well-known micronutrient that develops dental teeth and skeletal tissues (Chaudhari et al., 2024; Kar, 2022; Rashid et al., 2024a). Moreover, F<sup>-</sup> is also a ubiquitous pollutant found in different segments of the environment including the hydrosphere, atmosphere, lithosphere, and biosphere (Kar, 2022; Rashid et al., 2024a). Therefore, F<sup>-</sup> occurs in groundwater, surface water, soil, sediment, coal deposits, flora, fauna, industrial effluents, and geologic deposits (Kar, 2022; Kumar et al., 2023; Rashid et al., 2020). Earth's crust contains F<sup>-</sup> up to 0.06–0.09% and usually enters

the human organ through water ingestion (Boyet & Carlson, 2006; Noor et al., 2023). However, high F<sup>-</sup> groundwater ingestion is deleterious to human health, while an F<sup>-</sup> level within 0.5–1.5 mg/L would prevent dental cavities (Tokatlı et al., 2023), where higher F<sup>-</sup> > 1.5 mg/L develops community fluorosis in semiarid regions (Nizam et al., 2022; Rashid et al., 2023b).

High F<sup>-</sup> contamination in groundwater is a challenging task due to its geogenic and manmade sources (Rashid et al., 2023b; Tiwari et al., 2020). Most groundwater is contaminated with geogenic sources as compared to manmade sources (Abanyie et al., 2023; Agoro et al., 2020). Fluorosis problems mostly occur in Asian countries including Afghanistan (Hayat & Baba, 2017), Bangladesh (Jannat et al., 2022; Rahman et al., 2020), India (Adimalla et al., 2019; Jha & Tripathi, 2021; Sarkar et al., 2023), Pakistan (Rashid et al., 2020, 2023b, 2024a), Sri Lanka (Chandrajith et al., 2020; Young et al., 2011), China (Chen et al., 2017; Feng et al., 2020; Su et al., 2021), Myanmar (Bacquart et al., 2015), Japan (Amano et al., 2023), Italy (Parrone et al., 2020), Kenya (Mwiathi et al., 2022), Mexico (Ochoa-Rivero et al., 2023), North America (Abanyie et al., 2023), Saudi Arabia (Ghafar et al., 2014), Turkey (Yeşilnacar et al., 2016), and USA (McMahon et al., 2020).

Higher F<sup>-</sup> has been reported in the groundwater of Pakistan including Adenzai (Rashid et al., 2018), Dar-gai (Rashid et al., 2020), Mardan (Rashid et al., 2023b) Batkhela (Noor et al., 2022), Punjab plain (Khattak et al., 2022), Sindh Province Tharparkar (Ullah et al., 2023), Badin (Talpur et al., 2020), Umerkot (Jamali et al., 2023), Quetta (Rashid et al., 2024b; Ullah et al., 2022b), and Gilgit (Fatima et al., 2022). In Swabi, groundwater contamination occurs due to geochemical processes, ion exchange, semiarid conditions, industrial discharges, brick-making industries, coal combustion, agriculture runoff, inadequate sanitation, urbanization, and industrialization. Therefore, groundwater resources are highly contaminated with F<sup>-</sup> and HEs due to geogenic and anthropogenic inputs (Khattak et al., 2021). The geogenic sources include Ambela granite formations containing alkali granites, quartz-syenites, syenites, feldspathoidal syenites, and basic dikes, whereas the Koga complex contains syenites, fenites, feldspathoidal syenites, and carbonatites rocks (Khattak et al., 2021). The rock-water interaction, ion exchange, adsorption, desorption, dissolution of minerals, precipitation, and weathering of rocks releases F<sup>-</sup> in aquatic

systems (Rashid et al., 2022b; Wang et al., 2024). Excessive ingestion or deficiency of high and low levels of F<sup>-</sup> can potentially cause health risks in local people (Farag et al., 2023; Rashid et al., 2023a). Thus, the World Health Organization (WHO) declared the allowable limit F<sup>-</sup> 1.5 mg/L (WHO, 2011).

The water resource of Pakistan is depleting day by day at a faster rate. Thus, groundwater has declined both in quality and availability (Islam, 2023; Rashid et al., 2021, 2022b). The people predominantly used groundwater and surface water for domestic, industrial, drinking, and agricultural purposes (Rashid et al., 2023d; Ullah et al., 2023). The use of multivariate statistics and geochemical modeling techniques is useful in the identification of pollution problems that occur in aquatic systems (Rashid et al., 2019; Ullah et al., 2022a). We used different multivariate tools like principal component analysis (PCA), factor analysis (FA), agglomerative hierarchical cluster analysis (AHCA), and multilinear regression (MLR) (Rashid et al., 2020, 2023d). These statistical tools determined the potential contamination sources, percentile contribution, similarity, and dissimilarity indexing (Rashid et al., 2022a). The use of a geographic information system (GIS) is essential for geological, spatial distribution, and vulnerability mapping in groundwater (Rashid et al., 2019, 2023b).

In the above discussions, we studied groundwater contamination with high F<sup>-</sup> groundwater emanating from geogenic and anthropogenic inputs, source apportionment, health risks, and spatial distribution. This study compiles groundwater and surface contamination around Ambela and Koga complex formations and industrial settings in Swabi, Pakistan. The aim of this study was (i) to evaluate the high and low F<sup>-</sup> levels in groundwater and surface water and compare their geochemical characteristics of groundwater quality utilization for domestic and drinking purposes, (ii) to create a spatial distribution map of F<sup>-</sup> abundance mapping deciphering potentially vulnerable zones, and (iii) to examine human health risks through oral ingestion of F<sup>-</sup> contaminated groundwater.

## Material and methods

### Study area and geology

District Swabi lies between the Indus and Kabul river basins with an elevation from 300 to 650 m.

Geographically, Swabi lies between 34°20'00" to 33°50'00" N and 72°40'00" to 72°10'00" E (Fig. 1). The area is located in the northeastern part of Khyber Pakhtunkhwa (KPK) province occupying an area of 1543 km<sup>2</sup>. The northern side is occupied by Buner, the eastern side by Haripur, the southern side by Attack, and the western side by Mardan and Nowshera districts (Khattak et al., 2021).

The dominant geological units in the study area include Shewa, Ambela, and Warsak complexes and quaternary alluvium. The granitic rocks of Ambela and Koga are the predominant lithological units exposed in the study area. In a few places, metasedimentary rocks of the Paleozoic age are also present. Shah and Danishwar (2003) investigated the Ambela granite complex in detail and reported the rock units such as alkali granites, syenites, quartz syenites, basic dikes, and feldspathoidal syenite (Shah & Danishwar, 2003). They also described detailed petrographic features and the mineralogy of rocks from these regions. Their study indicated that most of the exposed rocks of the Ambela and Koga complex contain hornblende, fluorite, micas, and tourmaline minerals. Hence, the granitic rocks are found to be the major source of fluorite and the release of high concentrations of F<sup>-</sup> to the surrounding environment. The quaternary alluvium near streams and rivers might accumulate high F<sup>-</sup> from upstream granitic and Paleozoic rocks, especially where groundwater interacts with these formations. Furthermore, the Ambela and Koga formations contain potential F-bearing minerals which can lead to an excess of F<sup>-</sup> in the rocks, soil, surface, and groundwater (Shah & Danishwar, 2003).

### Geological composition of rocks containing fluoride

Swabi district lies in the northwestern side of Pakistan, within the foothills of the Himalayan Mountains. Geologically, the area is diverse, featuring sedimentary, igneous, and metamorphic rock formations. Sedimentary rocks include limestone, sandstone, and shale which contain F-bearing minerals, viz. fluorite (CaF<sub>2</sub>) or apatite (Ca<sub>5</sub>(PO<sub>4</sub>)<sub>3</sub>(F, Cl, OH)), whereas igneous rocks include intrusions of granite rocks which contribute F-enriched minerals such as biotite and hornblende to aquifers. On the other side, metamorphic formations, including schists and gneisses, contain F<sup>-</sup> in trace

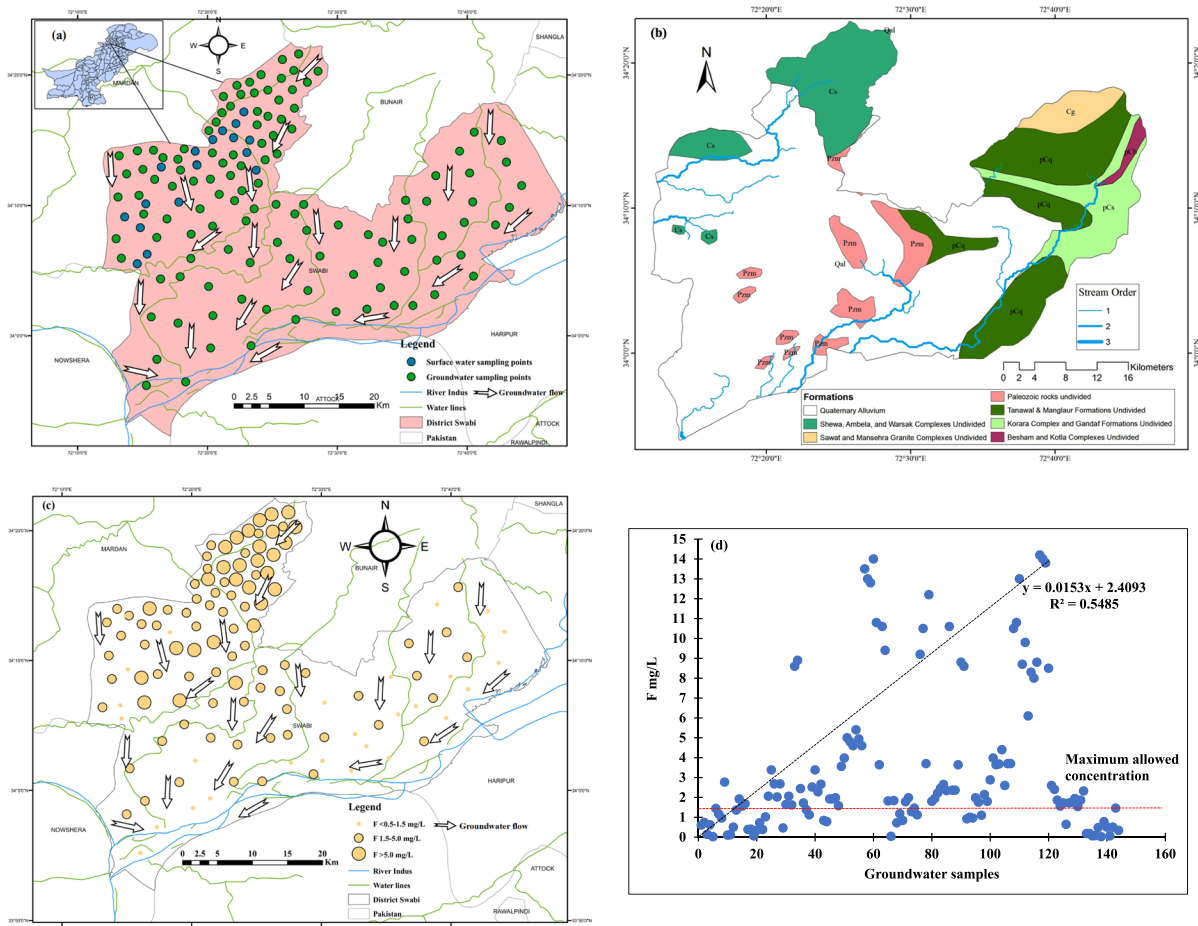
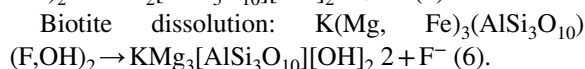
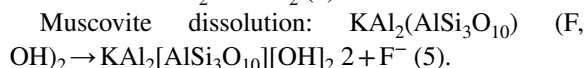
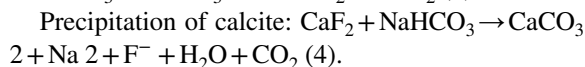
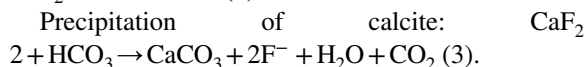


**Fig. 1** **a** Groundwater, and surface water sampling points, **b** geological formations modified from Chaudhry et al., 1982, **c** iso-concentrations model showing low, moderate, and high F<sup>-</sup>

amounts. To better understand the F<sup>-</sup> prevalence in the groundwater, see the following chemical reactions occurring in the aquifers.



Dissolution and precipitation of fluorite:  $\text{CaF}_2 \rightarrow \text{Ca}^{2+} + 2\text{F}^-$  (2).



concentrations, and **d** F<sup>-</sup> values determined maximum allowable limit in District Swabi, Pakistan

#### Groundwater sampling analysis

A total of 126 groundwater and 18 surface waters were collected from district Swabi, in July 2022. Groundwater samples were gathered from dug-well, tubewell, and handpump using a random sampling strategy. The collected samples were evaluated for physicochemical parameters and major ions. Therefore, 120-mL plastic bottles were used to assemble water samples. Each sample was gathered in two separate polyethylene bottles; one dataset was utilized for chemical tests (acidified with 3–4 drops of ultrapure HNO<sub>3</sub> with 65% purity) and the second dataset for physical tests (non-acidified). All water samples were stabilized by chemical additives and sample

filtration, avoiding aeration and exposure to sunlight and maintaining sample temperature at 4 °C. We used Whitman filter paper 0.45 µm to remove unwanted materials to protect sophisticated instruments such as atomic absorption spectrophotometers. The physical variables including EC, pH, and TDS were evaluated in situ by pH meter, electrochemical analyzer, and geographic coordinates using a global positioning system (GPS), respectively. F<sup>-</sup> content in groundwater and surface water was tested by HACH DR 2800 spectrophotometer, whereas NO<sub>2</sub><sup>-</sup>, NO<sub>3</sub><sup>-</sup>, and SO<sub>4</sub><sup>2-</sup> were tested by DR2-800 spectrophotometer, Cl<sup>-</sup> was tested by the Mohr method, and HCO<sub>3</sub><sup>-</sup> was measured using titration methods. The chemical variables such as Mg<sup>2+</sup>, Ca<sup>2+</sup>, K<sup>+</sup>, and Na<sup>+</sup> were analyzed via inductively coupled plasma mass spectrometry (ICP-MS Nexion 350X ICPMS Perkin Elmer Technologies, USA) having a detection limit of 0.01 µg/L.

#### Fluoride pollution index (FPI)

We measured the F<sup>-</sup> pollution index (FPI) using Eq. (1) (Rehman et al., 2022). Here, Table S1 determined the assigned weightage for the estimation of FPI values (Table S1).

$$\text{FPI} = \frac{\text{Wf} + \text{WHCO}_3 + \text{WNa/Ca} + \text{WpH}}{N} \quad (1)$$

Here, Wf determined the weight of F<sup>-</sup>, WHCO<sub>3</sub><sup>-</sup> represented the weight assigned to HCO<sub>3</sub><sup>-</sup>, and WNa/Ca showed the weight allotted to Na<sup>+</sup> and Ca<sup>2+</sup>, whereas WpH=weight allocated to pH as shown in Table S1. Here, N showed a total number of geochemical parameters in the water sample.

#### Saturation indices

The saturation indices in terms of mineral phase in drinking water were measured using PHREEQC Interactive 3.7.3–15968 and the WATEQF database, following Eq. (2).

$$\text{SI} = \text{Log} \frac{\text{IAP}}{\text{KT}} \quad (2)$$

#### Health risk assessment

Groundwater is exposed to a variety of potential contaminants including fluoride which causes health risks in semiarid conditions. Here, we measured the non-carcinogenic risks originating from high F<sup>-</sup> groundwater consumed by local people (Rashid et al., 2020). The chronic daily intake (CDI) of F<sup>-</sup> in groundwater was assessed in mg/kg/day based on exposure to F-contaminated water. Thus, non-carcinogenic risks were measured using Eq. (3) (CDI) and (4) (HQ), as defined by EPA (2001).

$$\text{CDI} = \frac{C \times \text{IR} \times \text{ED} \times \text{EF}}{\text{BW} \times \text{AT}} \quad (3)$$

where C represents the F<sup>-</sup> values in groundwater sample (mg/L), IR characterizes the daily ingestion rate (L/day) for adults=2 L/day and children=1 L/day (Rashid et al., 2023d), EF shows the exposure frequency that is 365 days/year, ED denotes exposure duration (adults=30 years and children=12 years), BW determines average body weight for children is 15 kg and for adult is 70 kg, and AT denotes average exposure time for adults is 10,950 days and children is 5380 days.

$$\text{HQ} = \frac{\text{CDI}}{\text{RFD}} \quad (4)$$

where HQ characterizes the hazard quotient, and RFD shows reference dose values for F<sup>-</sup> which is 0.06 mg/kg/day. Here, HQ values > 1.0 cause significant risks for local people consuming high F<sup>-</sup> water, while HQ values < 1 are considered safe (Rashid et al., 2020).

#### Statistical analysis

The groundwater of district Swabi is statistically analyzed for physicochemical variables. The statistical overviews include minimum, maximum, mean, and standard deviation concentration. We used XLSTAT 2022, IBM-SPSS 2022, Origin 2023b, and Microsoft Excel 2013 to calculate descriptive statistics, Pearson correlation, PCA, MLR, FA, and CA. However, ArcGIS 10.7 was used to study area, geological settings, and spatial distribution models.

The Piper and Gibbs plot was employed for the development of groundwater types and geochemical control mechanisms (Alharbi & Zaidi, 2018; Gibbs, 1977). Here, cations ( $\text{Ca}^{2+}$ ,  $\text{Mg}^{2+}$ , and  $\text{Na}^+$ ) are plotted against anions ( $\text{Cl}^-$ ,  $\text{SO}_4^{2-}$ , and  $\text{HCO}_3^- + \text{CO}_3^{2-}$ ) (Rashid et al., 2022b; Ullah et al., 2022a).

#### Groundwater quality control, assurance, and ion balance error

We have collected groundwater in duplicate, and their mean values were interpreted in the final results. Quality control (QC) and quality assurance (QA) were ensured by reagent blinks and laboratory standards for physicochemical analysis and quality assurance determining strategies for water maintenance, reproducibility, reliability, and data quality. The ionic charge balance error calculated for this study determined the precision and accuracy of water data (Rashid et al., 2020, 2023b). Here, anions and cations in groundwater were calculated as meq/L observed within  $\pm 5\%$  error; see Eq. 5.

$$\text{IBCE} = \frac{(\sum \text{Cations} - \sum \text{Anions})}{(\sum \text{Cations} + \sum \text{Anions})} \times 100 \quad (5)$$

## Results and discussion

### Geochemical composition of groundwater

Table 1 summarizes the groundwater and surface water parameters and their comparison with WHO recommended limits (Table 1) (WHO, 2011). The pH of the groundwater was many-fold higher than surface water in the entire region.

The range values of pH in groundwater were 7.1–11.7, and surface water was 7.7–9.6, respectively. The TDS and electrical conductivity (EC) in groundwater ranged from 390.9 to 1663.6  $\mu\text{S}/\text{cm}$  and 280.0 to 1395.0, and surface water was 380.7–1361.1  $\mu\text{S}/\text{cm}$  and 270.0–1075.0 mg/L, respectively. The increasing abundance of major ions showed the following patterns:  $\text{Na} > \text{Ca} > \text{K} > \text{Mg}$  and  $\text{HCO}_3^- > \text{SO}_4^{2-} > \text{Cl}^- > \text{CO}_3^{2-} > \text{NO}_2^- > \text{NO}_3^- > \text{F}^-$ , respectively. In this study, pH in groundwater showed 53.17%, and in surface water 44.4%, which has exceeded the WHO allowable limit, whereas EC and TDS values in groundwater samples up to 90% and 14.2% and surface water 70% and 11.1% have exceeded the WHO allowable limit of 400  $\mu\text{S}/\text{cm}$ , and 1000 mg/L (WHO, 2011). Meanwhile,  $\text{HCO}_3^-$  54% groundwater and 11.1% surface water have surpassed the WHO limit of 500 mg/L. In this study, 75% of groundwater and 22.2% of surface water samples have exceeded the WHO limit of  $\text{F}^-$  1.5 mg/L. The

**Table 1** Statistical summary of surface and groundwater parameters in district Swabi, Pakistan

Statistic	Groundwater ( <i>n</i> = 126)				Surface water ( <i>n</i> = 18)				WHO limit
	Min	Max	Mean	SD	Min	Max	Mean	SD	
pH	7.1	11.7	8.8	1.2	7.6	9.6	8.4	0.6	6.5–9.5
EC	390.9	1664	760.1	336	381	1361	1016	191	400
TDS	280	1395	617	279	270	1075	845.6	125	1000
Resistivity	0.1	124	19.7	15.9	3.9	41.4	26.6	12.6	-
$\text{F}^-$	0.2	14.2	4.0	1.6	1.1	2.8	1	0.4	1.5
$\text{NO}_2^-$	2	29	9.9	4.8	6	19	8.3	3.3	3
$\text{NO}_3^-$	0.6	41.2	7.2	8.5	2.5	7.1	5.1	1.2	50
$\text{SO}_4^{2-}$	122	650	346.4	117	225	435	303.8	65.1	500
$\text{Cl}^-$	16.4	232.5	102.8	63.7	111	255	166.1	51.5	250
$\text{CO}_3^{2-}$	7.1	165.1	78.5	32.5	27.9	105	63.9	23.5	-
$\text{HCO}_3^-$	104.8	665	369.4	131	236	557	363.3	99.8	500
$\text{Ca}^{2+}$	11.8	120.8	24.8	12.9	12.4	25.7	19.9	4.3	100
$\text{Mg}^{2+}$	9.1	47.4	17.1	5.7	10.5	21.8	14.7	3.4	50
$\text{K}^+$	0.2	101.5	8.9	19.1	20.8	70.7	29.5	11.7	12
$\text{Na}^+$	16.1	542.4	259.7	111	211	370	282	52.8	200

SD standard deviation

major cations  $\text{Na}^+$  showed 75.3% groundwater and 11.1% surface water which has surpassed the WHO limit of 200 mg/L.

Groundwater and surface water samples recorded high TDS, EC, pH,  $\text{Na}^+$ , and  $\text{HCO}_3^-$  and lower  $\text{Ca}^{2+}$ ,  $\text{NO}_3^-$ , and  $\text{Mg}^{2+}$  aquifers. Geochemically, groundwater is controlled by the weathering of rocks, mineral dissolution, ion exchange, and water–rock interaction (Rashid et al., 2022a; Varol & Davraz, 2014). The geochemical composition and ionic strength of this study supported the results compiled by Rashid et al. (2020). Here, high values of  $\text{Na}^+$  take their origin from the weathering of alumino-silicate minerals (Rashid et al., 2020), whereas  $\text{F}^-$  coexists with high pH,  $\text{Na}^+$ , TDS, and  $\text{HCO}_3^-$ , and low  $\text{Mg}^{2+}$  and  $\text{Ca}^{2+}$  aquifers reveal geochemical evidence of  $\text{F}^-$  from host granitic rock in the aquifers (Rashid et al., 2020, 2023a).

The dominant cation was  $\text{Na}^+$ , and the anion was  $\text{HCO}_3^-$  in the aquifer system. Here, the mole ratio of  $\text{Na}^+/\text{Cl}^- \geq 1$  determined that dissociation of halite is accountable for  $\text{Na}^+$  release in drinking water. In this study,  $\text{Na}^+/\text{Cl}^- > 1$ ; then  $\text{Na}^+$  would originate from the dissolution of silicate mineral (An et al., 2023; Rashid et al., 2024a). Here, the mole ratio of Na/Cl of the present study ranged from 0.202 to 0.8 mg/L; therefore, halite and alumino-silicate mineral dissociation are accountable for  $\text{Na}^+$  enrichment in the aquifer system (Rashid et al., 2022a). The higher values of  $\text{HCO}_3^-$  in groundwater originated from mineral dissolution, inorganic decay, carbonate weathering, and organic matter (Jiang et al., 2023; Rashid et al., 2024a; Wallick, 1981). The geochemical findings of the current study were compared with the results of nearby areas in Pakistan (Rashid et al., 2022a, 2023b).

#### Distribution of fluoride

The  $\text{F}^-$  values in groundwater and surface water in district Swabi are significantly varied in the area. In this study, the range and mean  $\pm$  SD values of  $\text{F}^-$  in groundwater were  $0.2\text{--}14.2$  and  $4.0 \pm 1.6$ , and surface water was observed to be  $1.12\text{--}0.8$  and  $1.0 \pm 0.4$  mg/L, respectively (Table 1). Groundwater contributed 75.3%, and surface water of 22.2% samples had surpassed WHO guidelines of  $\text{F}^-$  1.5 mg/L. Table 2 reveals the  $\text{F}^-$  classification in groundwater based on vulnerability (Table 2). Here, a

**Table 2** Groundwater classifications based on fluoride risk index (FRI) in district Swabi, Pakistan

Fluoride ranges	Risk class	Number of samples	% of samples
$\leq 0.50$	Very low	21	14.58%
0.51–1.00	Low	13	9.02%
1.01–1.50	Moderate	13	9.02%
1.51–1.99	High	27	18.75%
2.00–2.50	Very high	13	9.03%
> 2.50	Extremely high	56	38.89%

risk-based classification determined the following six classes: very low  $\text{F}^- < 0.5$ , low 0.51–1.00, moderate 1.01–1.50, high 1.51–2.00, very high 2.002–2.50, and extremely high > 2.51 mg/L. The iso-concentration model revealed low, moderate, and high  $\text{F}^-$  showing contamination up to 73.3% in district Swabi (Fig. 1c).

Table S2 reveals classification of drinking water samples falls below 0.5, 0.5–1.5, 1.52–0.5, 2.5–4.0, 4.0–5.0, 5.0–10.0, and > 10.0 mg/L, reflecting 13.9%, 18.75%, 29.17%, 14.578%, 4.19%, 9.72%, and 10.42%, respectively. Here, 44 drinking water samples lie within WHO guidelines of  $\text{F}^-$  1.5 mg/L, and about a hundred samples overall have surpassed the WHO limit. Furthermore, the individual percent contamination of  $\text{F}^-$  in groundwater samples showed 75% contamination, and 22.2% in surface water. The distribution of  $\text{F}^-$  in drinking water is based on classification fluoride values which influences the dental and skeletal health of children and adults in the area (Table S2). Here, class-1 shows  $\text{F}^- < 0.5$  mg/L causes a dental cavity, class-2 reveals 0.5–1.5 mg/L and promotes skeletal tissues and teeth, and class-3 shows  $\text{F}^-$  1.52–0.5 mg/L develops dental fluorosis, whereas class-4 reflects  $\text{F}^-$  2.5–4.0 mg/L promotes severe dental fluorosis, class-5 shows 4.0–5.0 mg/L promotes dental and skeletal fluorosis in adult, class-6 shows  $\text{F}^-$  5.0–10.0 mg/L promotes skeletal fluorosis, and class-7 shows  $\text{F}^-$  > 10.0 mg/L reveals crippling community fluorosis in the entire community (Rashid et al., 2018, 2023a; Shaji et al., 2024).

High  $\text{F}^-$  groundwater in district Swabi occurs due to F-bearing minerals, ion exchange, aquifer sediment, and oxidizing conditions. Moreover,  $\text{F}^-$  contamination in the surface water originated from geogenic rocks, steel industrial effluents, coal

combustion, phosphate fertilizers, and atmospheric deposition (Rashid et al., 2020). In this study, the fluorite and dissolution of other F-bearing minerals, viz. apatite, mica, biotite, muscovite, and amphibole observed in the host Ambela granite and Koga complex formation along with aquifer sediment would potentially contaminate groundwater and surface water system (Rafiq & Jan, 1989). Moreover,  $F^-$  in surface water could also originate from parental host granite rocks and environmental settings including steel industrial effluents, coal combustion, and agriculture practices in the area (Rashid et al., 2023a).

$F^-$  has been found in the earth's crust with mean values of 557 mg/kg (Agoro et al., 2020).

The F-bearing minerals, viz. amphibole, biotite, apatite, and muscovite, substituted  $F^-$  with  $OH^-$  in oxidizing conditions (Sathe et al., 2021). Higher  $F^-$  content is also found in igneous rocks, viz. granite, carbonate, and pegmatite (Rashid et al., 2023b; Shaji et al., 2024).

#### Geochemical control mechanism

Gibbs plot was used to determine geochemical processes controlling the groundwater composition (Gibbs, 1970). The TDS values were plotted against mole ratios of  $Na/Ca + Na$  and  $Cl/HCO_3 + Cl$  (Fig. 2a, b). The results of the Gibbs plot showed three important controlling mechanisms: (1) weathering of rock, (2) atmospheric precipitation, and (3) evaporation. The geochemical composition reveals that 85% of groundwater and 50% of surface water is controlled by rock dominance, whereas 15% of groundwater samples and 50% of surface water are controlled by evaporation processes. Here, the precipitation process is negligible in the area. However, water–rock interaction, weathering of rock, aquifer sediments, ionic exchange, climatic conditions, water flow, and internal bedrock mineralogy can control the geochemical composition of water sources. The geochemical results of this study are compared with the geochemical findings of Rashid et al., (2023a, b, c, d) in the neighboring area of Mardan which are consistent and similar to our findings (Rashid et al., 2023b). The current study significantly understands the mineral enrichment in groundwater sources resulting from rock weathering and mineral dissolution. As a result, most groundwater sources are affected by rock

weathering and mineral dissolution, and few samples by evaporation are affected.

#### Geochemical facies using *Piper*, and Durov, and role of Schoeller diagram

The Piper diagram classifies groundwater and surface water into (a) calcium type, (b) no dominant type, (c) magnesium type, (d) sodium type, (e) bicarbonate type, (f) sulfate type, and (g) chloride type. Here, most of the cations occupied no dominant type, and anions were positioned at sulfate type. However, few samples occupied calcium-type and sodium-type water. Moreover, the final output of the Piper Trilinear diagram shows 2.1%  $CaHCO_3$  type, 22.9%  $NaCl$  type, 1.3% mixed  $CaNaHCO_3$ , 33.3% mixed  $CaMgCl_2$  type, 31.2%  $CaCl_2$  type water, and 9.0%  $NaHCO_3$  type, respectively. The increasing order of geochemical facies showed the following pattern:  $CaMgCl_2 > CaCl_2 > NaCl > NaHCO_3 > CaHCO_3 > CaNaHCO_3$ , respectively. Piper Trilinear diagram shows the geochemical composition of groundwater and surface water (Prema and Patil, 2022) (Fig. 2c). The majority of groundwater determined that  $CaNaHCO_3$ , 33.3% mixed  $CaMgCl_2$  type, is considered the dominant water type. It is observed that high  $Na^+$ ,  $HCO_3^-$ , and  $Cl^-$  under rock-weathering, ionic exchange, and evaporation processes would result in high  $F^-$  in groundwater.

Geochemical results of groundwater and surface water samples were plotted on Durov and Schoeller plot to understand hydro-chemical facies (Obrike et al., 2023). In this study, the Durov diagram showed major ions, hydro-chemical facies along with TDS and pH values in groundwater systems (Fig. 2d). The groundwater samples with pH values ranged from 7.1 to 11.7, and TDS values were 100–300 mg/L. The lower pH and TDS values show enrichment of  $HCO_3^-$  salts with  $Ca^{2+}$  and  $Mg^{2+}$ . When groundwater samples are enriched with soluble  $Cl^-$  and  $SO_4^{2-}$  salts of  $Na^+$  and  $Mg^{2+}$ , their mineralization is increased from 500 to 1000 mg/L. The TDS values in the Durov diagram ranged from 280 to 800 mg/L, which indicates that the groundwater is mainly composed of mixed  $Cl^-$  and  $SO_4^{2-}$  types. Durov diagram represents groundwater samples with high values of  $HCO_3^-$ ,  $Na^+$ , and  $K^+$  and lower values of  $Mg^{2+}$  and  $Ca^{2+}$  in the aquifers (Rashid et al., 2022a).

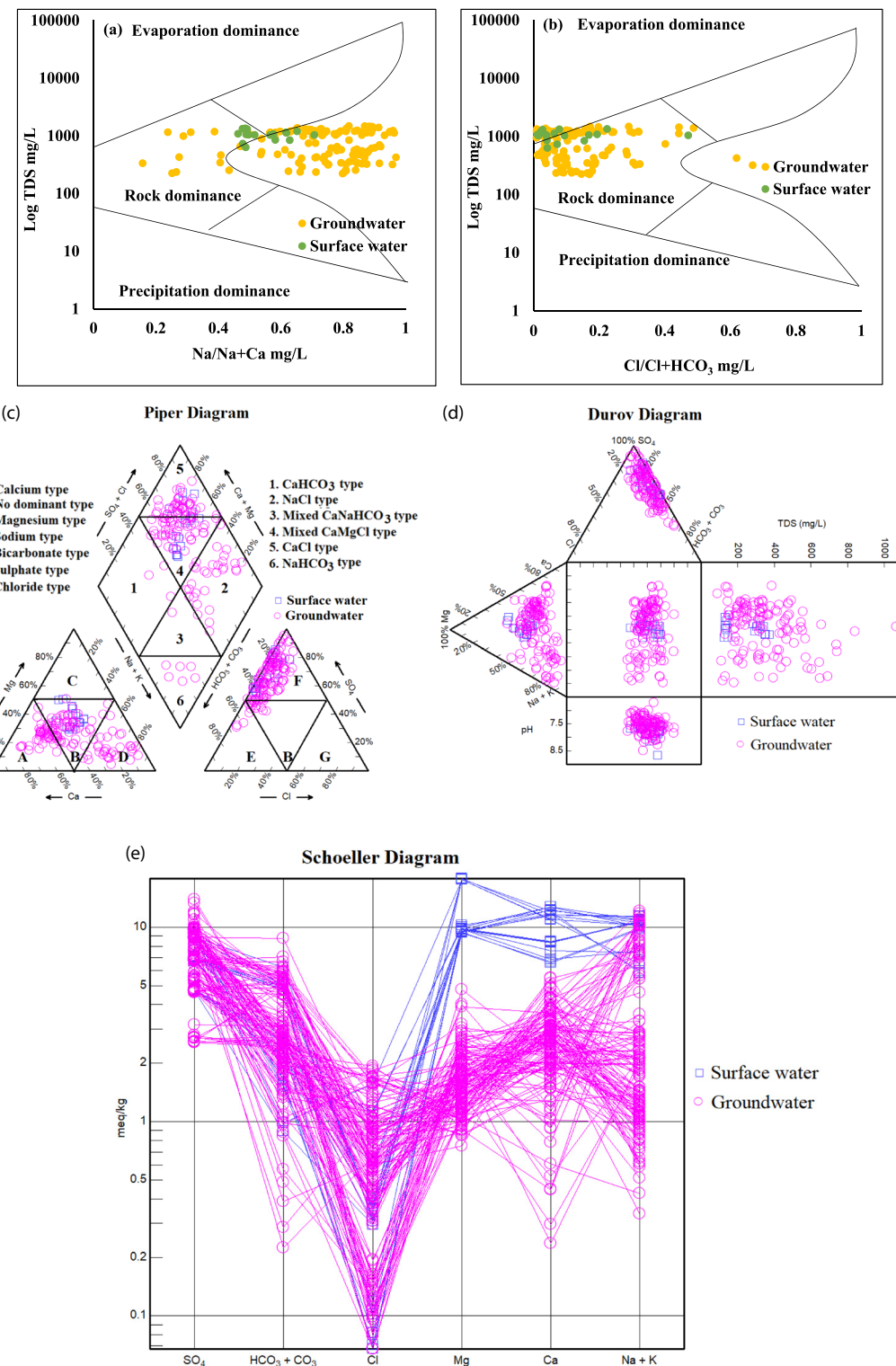


**Fig. 2** Geochemical control mechanisms; **a** major cations vs. log TDS, **b** major anions vs. log TDS, **c** Piper diagram, **d** Durov, and **e** Schoeller diagram in groundwater of District Swabi, Pakistan

Schoeller plot (1955) shows the variability of major ions in the groundwater samples (Singh & Kshetrimayum, 2021) (Fig. 2e). The Schoeller diagram (Fig. 2e) shows that  $\text{Na}^+$  and  $\text{HCO}_3^-$  are dominating, whereas  $\text{K}^+$ ,  $\text{Ca}^{2+}$ ,  $\text{Mg}^{2+}$ ,  $\text{Cl}^-$ , and  $\text{SO}_4^{2-}$  vary in the groundwater samples. The Durov and Schoeller plot illustrated the dominancy of  $\text{HCO}_3^-$ ,  $\text{Cl}^-$ ,  $\text{Na}^+$ ,  $\text{K}^+$ ,  $\text{Ca}^{2+}$ , and  $\text{Mg}^{2+}$ . Thus, Durov and Schoeller's plot determined the geochemical control mechanisms of aquifer compositions.

#### Pearson correlation and inter-elemental relationship in groundwater and surface water

Correlation coefficient analysis determined the inter-relationship between water variables. In this study, the correlation is significant  $r < 0.5$ .

Here, the groundwater variables with positive correlation suggest a common source, while negative correlation indicates different sources (Rashid et al., 2018). The correlation coefficient relation showed the following strong correlation pairs: pH and F ( $r=0.62$ ), pH and  $\text{HCO}_3$  ( $r=0.45$ ), pH and Na ( $r=0.36$ ) and pH and  $\text{NO}_3$  ( $r=-0.37$ ), EC and TDS ( $r=0.45$ ), EC and  $\text{NO}_3$  ( $r=0.47$ ), EC and  $\text{SO}_4$  ( $r=0.32$ ), F and  $\text{HCO}_3$  ( $r=0.76$ ), and F, and Na ( $r=0.48$ ) and F and  $\text{NO}_3$  ( $r=-0.44$ ),  $\text{NO}_3$  and Ca ( $r=0.41$ ),  $\text{NO}_3$  and Mg ( $r=0.37$ ) and  $\text{NO}_3$  and  $\text{HCO}_3$  ( $r=-0.43$ ),  $\text{HCO}_3$  and Na ( $r=0.54$ ), Ca and Mg ( $r=0.60$ ), and surface water were pH and F ( $r=0.41$ ), pH and  $\text{NO}_3$  ( $r=0.42$ ), pH, and  $\text{SO}_4$  ( $r=0.40$ ), pH and  $\text{CO}_3$  ( $r=0.44$ ) EC and  $\text{SO}_4$  ( $r=-0.47$ ) and EC and  $\text{HCO}_3$  ( $r=-0.39$ ). TDS and Na ( $r=-0.37$ ), resistivity and  $\text{NO}_3$  ( $r=-0.47$ ), F and  $\text{NO}_2$  ( $r=0.53$ ), F and Na ( $r=-0.42$ ), F and Ca ( $r=-0.57$ ), F and Mg ( $r=-0.46$ ) and F and Na ( $r=-0.37$ ),  $\text{SO}_4$  and Na ( $r=-0.60$ ), Cl and Na ( $r=-0.44$ ), Ca and Mg ( $r=0.83$ ) (Fig. S1a, b), respectively. The strong positive and negative correlation parameters with fluoride promoted the release of high  $\text{F}^-$  in the aquifer systems which later on caused health risks to the local population.

#### Weathering and dissolution of carbonate, silicate, and evaporite dissolution

The groundwater and surface water containing a high amount of  $\text{Ca}^{2+}$  and  $\text{Mg}^{2+}$  reveal that carbonate rock minerals dissolve in the aquifers (Fig. 3a, b). Water

penetration and inward flow dissolve  $\text{CaCO}_3$ , and  $\text{Ca}-\text{Mg}(\text{CO}_3)_2$  minerals enhance the  $\text{Ca}^{2+}$  and  $\text{Mg}^{2+}$  in aquatic ecosystems. The scatterplot of  $\text{Ca} + \text{Mg}$  vs.  $\text{HCO}_3 + \text{SO}_4$  showed that Ca and Mg would be slightly lower than  $\text{HCO}_3 + \text{SO}_4$  values. The findings of  $\text{Ca} + \text{Mg}$  vs.  $\text{HCO}_3 + \text{SO}_4$  plot were compared with Rashid et al. (2022a). The ionic strength of  $\text{Ca}^{2+}$  and  $\text{Mg}^{2+}$  falls above equiline resulting in carbonate rock-weathering mechanisms. The chemical variables fall nearer to equiline reveals from carbonate-weathering, and contrasting effects are determined by silicate-weathering. To understand the mechanisms, see Eqs. 7–10 showing silicate weathering. In this study, the carbonate weathering is predominately determined by the  $\text{Ca} + \text{Mg}$  vs.  $\text{HCO}_3 + \text{SO}_4$  plot (Fig. 3a, b). The findings show that samples that fall above and around the equiline determined carbonate weathering, and those that fall below the equiline showed silicate weathering. Thus, carbonate and silicate weathering are the prime sources of  $\text{Ca}^{2+}$  and  $\text{Mg}^{2+}$  in aquatic ecosystems. In this study, some useful plots show carbonate, evaporite, and silicate weathering dissolution. Figure 3a shows the association between  $\text{HCO}_3/\text{Na}$  against  $\text{Ca}/\text{Na}$ . Figure 3b reveals a link of  $\text{Mg}/\text{Na}$  against  $\text{Ca}/\text{Na}$  to document carbonate, evaporite dissolution, and silicate weathering (Fig. 3a, b).

Furthermore, cations in the aquatic system also originated from silicate weathering (Jenckes et al., 2024). Here, the  $\text{Na} + \text{K}$  vs. total cations plot shows that all surface water and a few groundwater samples fall above the  $\text{Na} + \text{K} = 0.5 \text{ TZ}^+$  line (Changsheng et al., 2022). Thus, cations in the aquifer are highly enriched as a result of silicate weathering. Here,  $\text{Na}^+$  and  $\text{K}^+$  are about 56% of the total cations (Fig. 3c). The low concentration of  $\text{Na}^+$  and  $\text{K}^+$  occurs due to  $\text{Ca}/\text{Na}$  ratio that would further decrease  $\text{Na}^+$  values in aquifers. Both carbonate and silicate weathering show the dominancy of  $\text{HCO}_3^-$  species. However, if  $\text{CO}_3^{2-}$  occurs along the flow path, then rain and irrigated water interact with  $\text{CO}_2$ , and  $\text{H}_2\text{CO}_3$  would release  $\text{HCO}_3^-$  in aquifers. During groundwater recharge,  $\text{Ca}^{2+}$  and  $\text{HCO}_3^-$  trigger into groundwater (Fig. 3c). Similarly, the silicate weathering further increases  $\text{HCO}_3^-$  values in the groundwater as a result of  $\text{F}^-$  release into the aquifer. Therefore, the  $\text{Na}$  vs.  $\text{HCO}_3$  plot reveals silicate weathering (see Eq. 14). Furthermore, the carbonate, evaporite dissolution, and silicate weathering are influencing the aquatic system (Fig. 3). Here, the  $R^2$  values for (a)  $\text{HCO}_3/\text{Na}$  vs.  $\text{Ca}/\text{Na}$

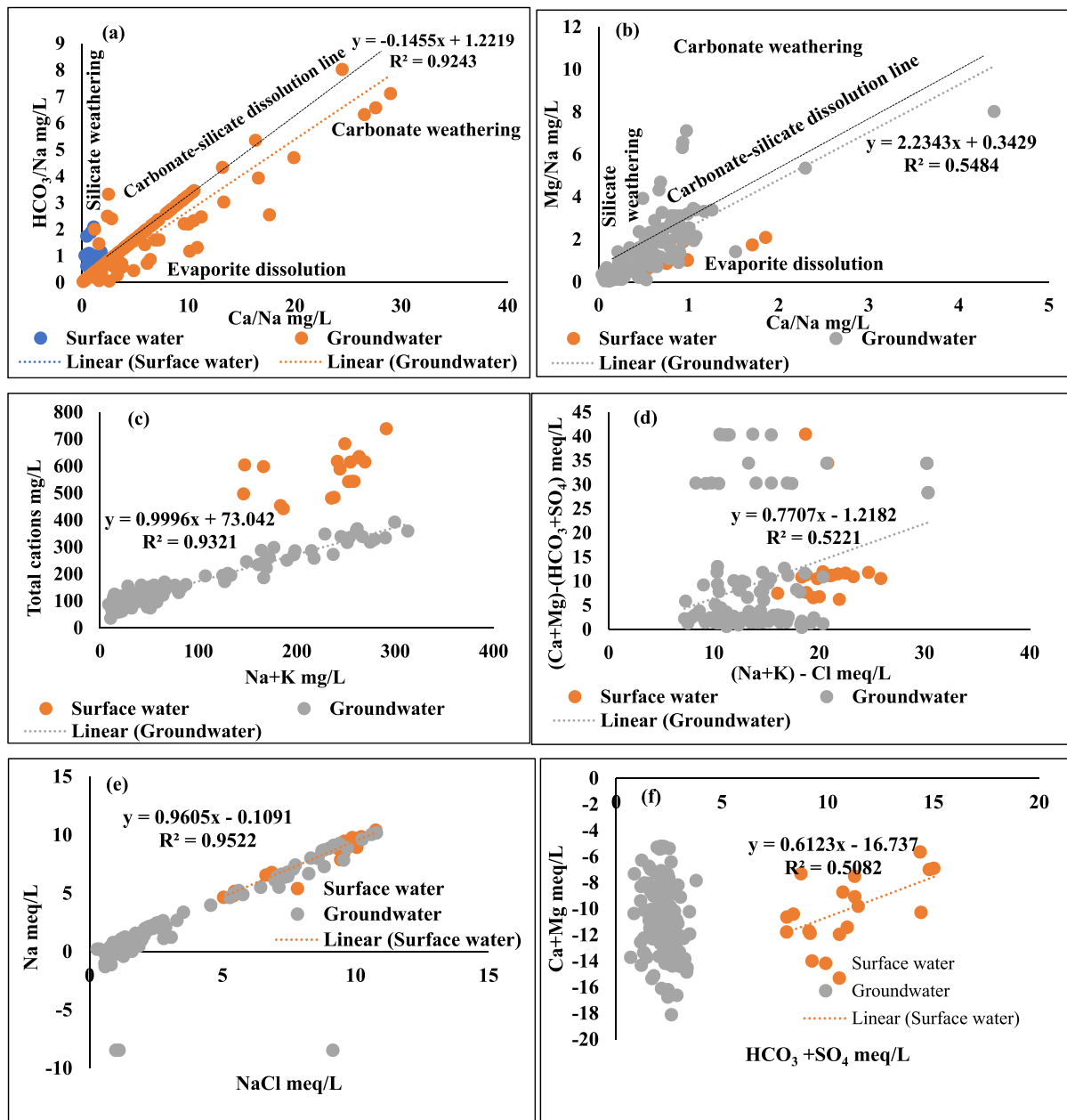


**Fig. 3** Cross-plot reveals influences on geochemical processes; **a**  $\text{HCO}_3/\text{Na}$  vs.  $\text{Ca}/\text{Na}$ ; **b**  $\text{Mg}/\text{Na}$  vs.  $\text{Ca}/\text{Na}$  indicated evaporite dissolution, silicate, and carbonate weathering;

ing; **c** total cations vs.  $\text{Na}+\text{K}$ ; **d**  $(\text{Ca}+\text{Mg})-(\text{HCO}_3+\text{SO}_4)$  vs.  $(\text{Na}+\text{K})-\text{Cl}$ ; **e**  $\text{Na}^+$  vs.  $\text{NaCl}$  meq/L; and **f**  $\text{Ca}+\text{Mg}$  vs.  $\text{HCO}_3+\text{SO}_4$  meq/L in aquatic system

Na, (b)  $\text{Mg}/\text{Na}$  vs.  $\text{Ca}/\text{Na}$  indicated evaporite dissolution, silicate, and carbonate weathering; (c) total cations vs.  $\text{Na}+\text{K}$ , (d)  $(\text{Ca}+\text{Mg})-(\text{HCO}_3+\text{SO}_4)$  vs.  $(\text{Na}+\text{K})-\text{Cl}$ , (e)  $\text{Na}^+$  vs.  $\text{NaCl}$  meq/L, and (f)  $\text{Ca}+\text{Mg}$  vs.  $\text{HCO}_3+\text{SO}_4$  in aquatic systems were 0.92, 0.54, 0.93, 0.52, 0.95, and 0.51, respectively (Fig. 3a-f).

#### Human health risk assessment

The range and mean  $\pm$  SD values of  $\text{F}^-$  in groundwater were 0.0202–0.770 and  $0.0202 \pm 0.770$ , and in surface water 0.020–14.200 and  $3.893 \pm 3.761$ , respectively. Here, chronic daily ingestion (CDI), hazard

quotient (HQ), and total health indices (THI) values for children and adults are presented in Table 3. In this study, the CDI values for children ranged from 0.001 to 0.981 in groundwater and 0.001 to 0.179 in surface water, and for adults were 0.001–0.406 and 0.001–0.079, respectively.

The HQ values of children ranged from 0.022 to 15.29 in groundwater and 0.0222 to 0.983 in surface water, and for adults were 0.10–6.762, and 0.010–1.319, respectively. The total health indices (THI) values were 0.011–7.168 in groundwater and 0.011–1.398 in surface water, respectively. In the case of children, 77.08% of samples exceeded the maximum allowed value of  $HQ > 1$ , and in the case of adults 46.52%  $HQ > 1$ . In this study, fluoride causes severe health issues in children as compared to adults. Overall, the fluoride toxicity in groundwater ingestion with high  $F^-$  concentrations causes community fluorosis problems in Swabi, Pakistan. The community fluorosis indexing (CFI) values showed different classes of investigated people in the study area (Fig. 4a). Overall, CFI exceeded 0.6 resulting in dental and skeletal fluorosis (Rashid et al., 2018).

### Spatial distribution pattern of fluoride

The distribution of fluoride is shown in groundwater and surface water systems; see Fig. 4b, c. The spatial distribution model of  $F^-$  showed substantial variations throughout the entire region at  $P < 0.05$ ,  $\text{sig} < 0.001$ . Here,  $F^-$  in groundwater, and surface water is spatially distributed within the range of 0.2–14.2 and 1.12–8 mg/L (Fig. 4b, c). Groundwater wells revealed 75.3% and surface water 22.2%  $F^-$  contamination due to natural and manmade activities in the entire region. The fluctuations in the distribution of  $F^-$  in the entire region resulted from mineral dissolution around hosted Ambela and Koga complex

formations. Furthermore, the lowest  $F^-$  0.2 mg/L and the highest 14.2 mg/L were observed in groundwater. The geospatial maps of  $F^-$  displayed the lowest, lower, moderate, polluted, and severely polluted class based on the vulnerability, and enrichment of  $F^-$  in the groundwater, and surface water in the region.

The geospatial maps of fluoride displayed the lowest (0.042–0.8), lower (2.9–5.6), moderate (5.7–8.4), polluted (8.5–11.0), and severely polluted (12.0–14.0) groups based on the vulnerability, and enrichment of  $F^-$  in the groundwater, and surface water in the area. Here,  $F^-$  are more noticeable around the Naranji and Parmoli areas showing the vulnerability of groundwater and surface water deterioration in the area. However, the  $F^-$  vulnerability in groundwater sources decreases away from Naranji towards Shera Gund, Kamardanad, Shardara, Tutali, Shawa, Shejana, Kalukhan, Dagai, Yaru hussain, Shahdheri, Sara cheena, and Muslimabad, respectively.

### Mineral phases in groundwater and surface water system

Figure 5 compiles the saturation indices (SI) values of drinking water sources displaying under-saturation and saturation showing precipitation and dissolution of minerals during equilibrium phases at 25 °C (Fig. 5a–c). The SI values of anhydrite, aragonite, calcite, dolomite, epsomite, fluorite, huntite, magnesite, mirabilite, natron, and nesquehonite vs. Ca, F, and TDS were plotted (Fig. 5a–c). In this study, aragonite, calcite, dolomite, fluorite, huntite, magnesite, and natron showed saturation, while anhydrite, epsomite, mirabilite, and nesquehonite determined under-saturation at equilibrium phases in the area. The saturation of fluorite minerals in the entire region reveals that groundwater is significantly contaminated

**Table 3** Chronic daily ingestion (CDI) and hazard quotient (HQ) determination for adults and children of district Swabi, Pakistan

S. no	Groundwater ( $n=126$ )		Surface water ( $n=18$ )	
	Range	Mean $\pm$ SD	Range	Mean $\pm$ SD
$F^-$ mg/L	0.020–14.200	$3.893 \pm 3.761$	0.020–2.770	$0.915 \pm 0.753$
CDI children	0.001–0.918	$0.223 \pm 0.243$	0.001–0.179	$0.059 \pm 0.049$
HQ children	0.022–15.292	$3.721 \pm 4.050$	0.022–2.983	$0.985 \pm 0.810$
CDI adult	0.001–0.406	$0.099 \pm 0.107$	0.001–0.079	$0.026 \pm 0.022$
HQ adult	0.010–6.762	$1.645 \pm 1.291$	0.010–1.319	$0.436 \pm 0.358$
THI	0.011–7.168	$1.744 \pm 1.398$	0.011–1.398	$0.452 \pm 0.380$

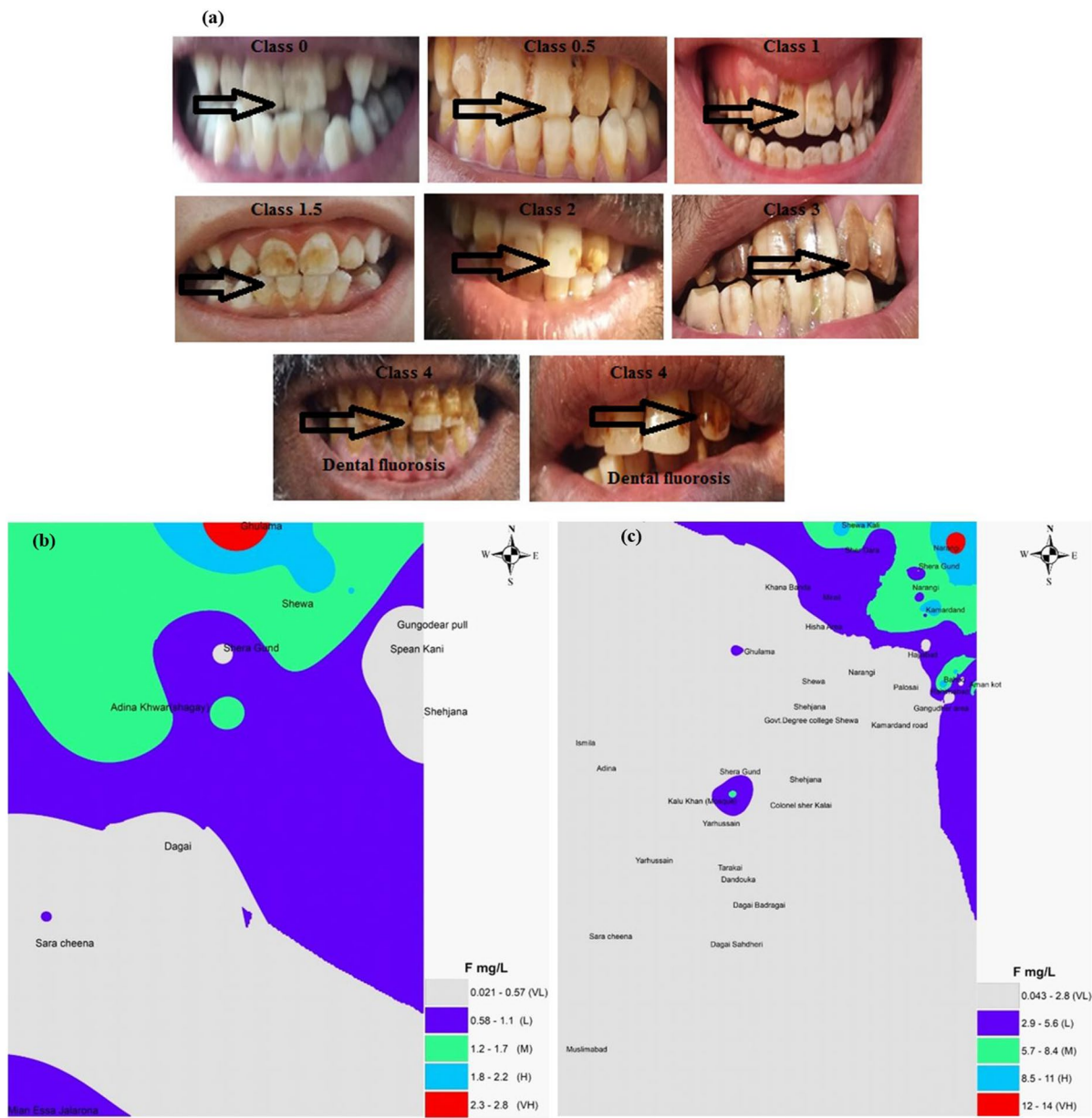


**Fig. 4** **a** Describe community fluorosis indexing (CFI), and dental fluorosis symptoms, **b**  $F^-$  distribution in surface water, and **c**  $F^-$  enrichment in groundwater determined very low, low, moderate, high, and very high class in District Swabi, Pakistan

with fluoride causing community fluorosis (Rashid et al., 2018).

#### Source apportionment

Principal component analysis and multilinear regression (PCA-MLR) were employed to analyze the groundwater in the district Swabi, Pakistan. Here,

PCA-MLR combined the inference of contamination sources and percentage contribution. In this study, the pollution load was arranged according to Rashid et al. (2020). The distinct percent contributions of loading factors were adjusted and multiplied by 100 with factor difference, then divided by the difference summation to get individual percent contribution (Khattak et al., 2021; Rashid et al., 2023b).

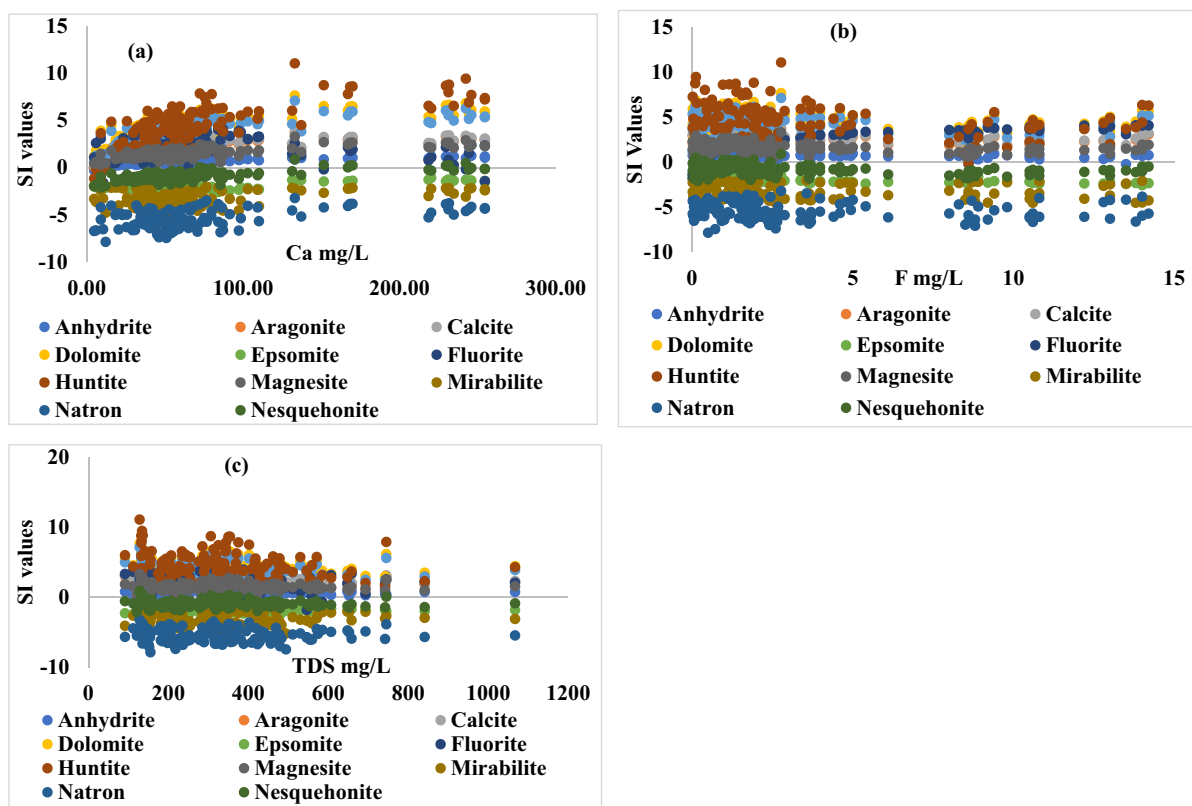


**Fig. 5** Mineral phases of physicochemical variables in groundwater; **a** SI values vs. Ca, **b** SI values vs. F, and **c** SI values vs. TDS

The results of PCA-MLR of 15 groundwater parameters in Swabi, Pakistan, were accumulated in five potential loading factors with a cumulative percentage  $> 74.8\%$  (Table 4.). Therefore, 15 loading factors overall were obtained after the varimax-rotation reduction dimension (Dinç & Güç, 2022) (Fig. 6a). The loading factors F1–F5 achieved 24.67%, 20.60%, 12.03%, 9.14%, and 8.34% contribution with eigenvalues 4.89, 2.82, 2.68, 1.58, and 1.17, respectively. The findings of PCA of the initial two factors assessed groundwater parameters as smaller and larger ellipses with a percentile contribution of 45.26%, and eigenvalues of 13.14 (Fig. 6b).

F1 described a 24.67% variation with an eigenvalue of 4.89 (Table 4. and Fig. 6a, b) and 36.25% contribution after MLR (Fig. 6c). F1 described a 24.67% variation showing significant loading for pH,  $\text{F}^-$ ,  $\text{CO}_3^{2-}$ ,  $\text{HCO}_3^-$ ,  $\text{K}^+$ , and  $\text{Na}^+$  with their correlation coefficient ( $r$ ) values being 0.56, 0.82, 0.66, 0.78, 0.60, and 0.71 and negated values for  $\text{Ca}^{2+}$  and  $\text{Mg}^{2+}$  being  $-0.82$ , and  $-0.86$ , respectively (Table 4.).

**Table 4** PCA results after the reduction dimension method for groundwater samples ( $n=144$ ) from Swabi, Pakistan

	F1	F2	F3	F4	F5
pH	<b>0.56</b>	0.25	<b>0.59</b>	-0.19	0.24
EC	0.10	<b>0.56</b>	0.45	0.23	0.47
TDS	0.02	<b>0.52</b>	0.40	0.32	0.39
$\text{F}^-$	<b>0.82</b>	<b>0.51</b>	<b>0.50</b>	0.46	0.08
$\text{NO}_2^-$	-0.11	-0.03	-0.31	0.27	<b>0.67</b>
$\text{NO}_3^-$	-0.45	-0.35	-0.40	<b>0.56</b>	<b>0.54</b>
$\text{SO}_4^{2-}$	0.46	-0.41	0.28	<b>0.52</b>	<b>0.52</b>
$\text{Cl}^-$	-0.41	0.15	<b>0.64</b>	-0.15	<b>0.50</b>
$\text{CO}_3^{2-}$	<b>0.66</b>	<b>0.62</b>	-0.21	0.37	0.01
$\text{HCO}_3^-$	<b>0.78</b>	<b>0.68</b>	-0.18	0.48	-0.08
$\text{Ca}^{2+}$	<b>-0.82</b>	<b>-0.59</b>	0.05	-0.06	0.09
$\text{Mg}^{2+}$	<b>-0.86</b>	<b>-0.50</b>	0.10	-0.20	0.06
$\text{K}^+$	<b>0.60</b>	0.20	<b>0.52</b>	0.20	-0.04
$\text{Na}^+$	<b>0.71</b>	<b>0.52</b>	0.26	0.53	-0.09
Eigenvalue	4.89	2.82	2.68	1.58	1.17
Variability (%)	24.67	20.60	12.03	9.14	8.34
Cumulative %	24.67	45.26	57.29	66.44	74.78

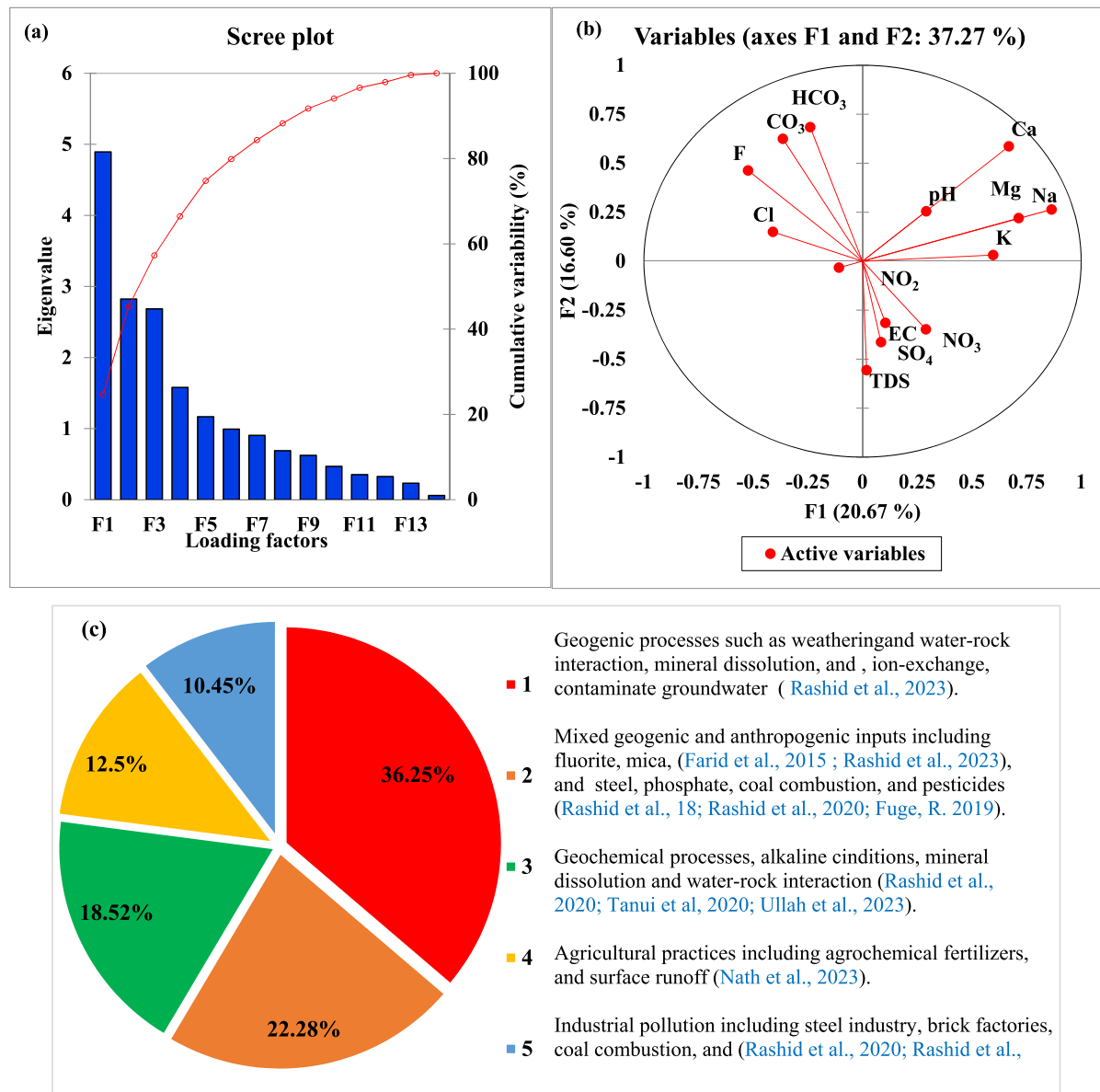


**Fig. 6** a Factors loading, b first two factors F1 and F2, and c percentile contribution after multilinear regression (MLR) analysis

In this study, high pH, F<sup>-</sup>, CO<sub>3</sub><sup>2-</sup>, HCO<sub>3</sub><sup>-</sup>, Ca<sup>2+</sup>, Mg<sup>2+</sup>, K<sup>+</sup>, and Na<sup>+</sup> resulted from water–rock interaction, rock-weathering, ion-exchange, and dissolution of fluorite, muscovite, biotite, calcite, dolomite, plagioclase, albite, and feldspar minerals (Rashid et al., 2023b; Xaza, 2020). However, pH in drinking water sources has a specific role in water composition, and mineral dissolution promoting fluoride mobilization, in groundwater systems (Li et al., 2022; Rashid et al.,

2022b; Ullah et al., 2023). Here, F1 characterizes the influences of geogenic processes and mineral prospects triggering the F<sup>-</sup> in the aquifers (Rashid et al., 2023b).

F2 elucidated 20.60% variability with 2.82 eigenvalues (Table 4. and Fig. 6a) and 22.28% after MLR contribution (Fig. 5c). F2 described for 20.60% variation with significant loading for EC, TDS, F<sup>-</sup>, CO<sub>3</sub>, HCO<sub>3</sub>, and Na<sup>+</sup> with coefficient *r* values were 0.56,

0.52, 0.51, 0.62, 0.68, and 0.52, and negated values for  $\text{Ca}^{2+}$  and  $\text{Mg}^{2+}$  were  $-0.59$  and  $-0.50$ , respectively. The EC in groundwater has resulted from leakage, alkaline conditions, and salinity (Farid et al., 2015), and TDS,  $\text{F}^-$ ,  $\text{CO}_3^{2-}$ ,  $\text{HCO}_3^-$ , and  $\text{Na}^+$  occur due to rock-weathering, fluoride-bearing minerals, carbonate weathering, organic matter, and minerals salts (Rashid et al., 2018). F2 showed mixed geogenic and anthropogenic sources including rock-weathering and dissolution of fluorite and mica, mineral (Farid et al., 2015; Rashid et al., 2023b) and steel, phosphate, coal combustion, and pesticides (Fuge, 2019; Rashid et al., 2020). Overall, F2 represented mixed geogenic and anthropogenic influences that deteriorated groundwater quality in the entire region.

Factor F3 represented 12.03% variability with 2.68 eigenvalues (Table 4. and Fig. 6a) and 18.52% contribution after MLR (Fig. 6c). F3 showed pH,  $\text{F}^-$ ,  $\text{Cl}^-$ , and  $\text{K}^+$  with coefficient  $r$  values were 0.59, 0.50, 0.64, and 0.52, respectively. The pH has a direct relation with semiarid and alkaline environmental conditions which influences groundwater chemistry markedly (Tanui et al., 2020; Ullah et al., 2023), whereas  $\text{K}^+$  and  $\text{Cl}^-$  in groundwater have resulted from sylvite salt (Rashid et al., 2022a).

F4 accounted for a 9.14% variation with 1.58 eigenvalues (Table 4. and Fig. 6a), and a 12.50% contribution after MLR (Fig. 6c). F4 revealed significant loading for  $\text{NO}_3^-$  and  $\text{SO}_4^{2-}$  with coefficient  $r$  values were 0.56 and 0.52, respectively. F4 revealed agriculture pollution resulting in  $\text{NO}_3^-$  and  $\text{SO}_4^{2-}$  contamination in the groundwater system of the area. Thus,  $\text{NO}_3^-$  and  $\text{SO}_4^{2-}$  contamination originated from agricultural practices including agrochemical fertilizers and surface runoff (Nath et al., 2023).

F5 showed an 8.34% variation with 1.17 eigenvalues and a 10.45% contribution after MLR (Table 4. and Fig. 6a and c). F5 described significant loading for  $\text{NO}_2^-$ ,  $\text{NO}_3^-$ ,  $\text{SO}_4^{2-}$ , and  $\text{Cl}^-$  with coefficient  $r$  values being 0.67, 0.54, 0.52, and 0.50, respectively. F5 explained industrial pollution including the steel industry, brick factories, and coal combustion resulting in  $\text{NO}_2^-$ ,  $\text{NO}_3^-$ ,  $\text{SO}_4^{2-}$ , and  $\text{Cl}^-$  contamination in drinking water sources of the area (Rashid et al., 2020, 2023b; Saeed et al., 2012).

Thus,  $\text{F}^-$  is present in host rock materials containing potential fluoride-bearing minerals, and its dissolution, water–rock interaction, and ion-exchange mechanisms trigger  $\text{F}^-$  in the groundwater of the

entire region. Additionally, mixed geogenic and anthropogenic inputs, along with agriculture fertilizers and industrial effluents, contributed to  $\text{F}^-$  contamination in the groundwater system.

## Conclusions

This study evaluated major ions,  $\text{F}^-$  contamination health risks, and their source apportionment using HHRA and PCA-MLR models in the groundwater of Swabi, Pakistan. Most shallow groundwater 75.3% and 22.3% surface water had exceeded the WHO guidelines of  $\text{F}^-$  1.5 mg/L. The high  $\text{F}^-$  groundwater is linked with high  $\text{HCO}_3^-$ ,  $\text{Na}^+$ ,  $\text{K}^+$ , and pH and depleted  $\text{Ca}^{2+}$  and  $\text{Mg}^{2+}$  content. Geochemically, groundwater chemistry is mainly controlled by rock weathering, ion exchange, and dissolution of minerals. The geochemical facies showed 33.3% mixed  $\text{CaMgCl}_2$  type, 31.2%  $\text{CaCl}_2$ , 22.9%  $\text{NaCl}$ , and 9.0%  $\text{NaHCO}_3$  type water. Mineral phases showed the dissolution of fluorite and precipitation of calcite and dolomite minerals promoting  $\text{F}^-$  prevalence in the aquifers. PCA-MLR model represented five potential sources for groundwater contamination. The FRI showed that 50% and the FPI revealed 48.73% of the population are in the high-risk category. Thus, FRI, FPI, and HHRA-model showed non-carcinogenic health concerns of  $\text{F}^-$  in groundwater systems. This study strongly recommended groundwater management and de-fluoridation techniques to reduce the risk of high  $\text{F}^-$  groundwater in the endemic region. Therefore, government and local authorities would take their prime responsibility to minimize human health concerns via de-fluoridation, and also residents need to utilize deep water for drinking and domestic demands.

**Acknowledgements** We are thankful to the Director of the National Centre of Excellence in Geology, University of Peshawar, for laboratory work and instrumental facilitation.

**Author contribution** Muhammad Tariq: conceptualization, methodology, writing—original draft. Abdur Rashid, Seema Anjum Khattak: field sampling and design lab protocol. Mohammad Tahir Shah: software analysis, validation. LiaqatAli: perform experimental work and software validation. Abdur Rashid and LiaqatAli: writing—review and editing, funding acquisition, supervision.

**Data availability** The data that has been used is confidential.

## Declarations

**Ethical approval** All authors have read, understood, and have complied as applicable with the statement on “Ethical responsibilities of Authors” as found in the Instructions for Authors.

**Consent to participate** Not applicable.

**Competing interests** The authors declare no competing interests.

## References

- Abanyie, S. K., Apea, O. B., Abagale, S. A., Amuah, E. E. Y. and Sunkari, E. D. (2023) Sources and factors influencing groundwater quality and associated health implications: A review. *Emerging Contaminants*: 100207.
- Adimalla, N., Marseatty, S. K. & Xu, P. (2019) Assessing groundwater quality and health risks of fluoride pollution in the Shasler Vagu (SV) watershed of Nalgonda, India. *Human and Ecological Risk Assessment: An International Journal*. <https://doi.org/10.1080/10807039.2019.1594154>
- Agoro, M. A., Adeniji, A. O., Adefisoye, M. A., & Okoh, O. O. (2020). Heavy metals in wastewater and sewage sludge from selected municipal treatment plants in Eastern Cape Province. *South Africa. Water*, 12(10), 2746.
- Alharbi, T. G., & Zaidi, F. K. (2018). Hydrochemical classification and multivariate statistical analysis of groundwater from Wadi Sahba Area in Central Saudi Arabia. *Arabian Journal of Geosciences*, 11, 1–10.
- Amano, H., Ichikawa, T., Fujimoto, K., & Nakagawa, K. (2023). Hydrogeochemical factors controlling the fluoride concentration in spring/groundwater in Aso caldera in the volcanic region, Japan. *Environmental Earth Sciences*, 82(13), 321.
- An, G., Kang, H., Fu, R., Xu, D., & Li, J. (2023). Investigation on the hydrogeochemical characteristics and controlling mechanisms of groundwater in the coastal aquifer. *Water*, 15(9), 1710.
- Ayub, M., Javed, H., Rashid, A., Khan, W. H., Javed, A., Sardar, T., Shah, G. M., Ahmad, A., Rinklebe, J. and Ahmad, P. (2024) Hydrogeochemical properties, source provenance, distribution, and health risk of high fluoride groundwater: Geochemical control, and source apportionment. *Environmental Pollution*: 125000.
- Bacquart, T., Frisbie, S., Mitchell, E., Grigg, L., Cole, C., Small, C., & Sarkar, B. (2015). Multiple inorganic toxic substances contaminating the groundwater of Myingyan Township, Myanmar: Arsenic, manganese, fluoride, iron, and uranium. *Science of the Total Environment*, 517, 232–245.
- Boyett, M., & Carlson, R. W. (2006). A new geochemical model for the Earth's mantle inferred from 146Sm–142Nd systematics. *Earth and Planetary Science Letters*, 250(1–2), 254–268.
- Cannas, D., Loi, E., Serra, M., Firinu, D., Valera, P., & Zavattari, P. (2020). Relevance of essential trace elements in nutrition and drinking water for human health and autoimmune disease risk. *Nutrients*, 12(7), 2074.
- Chandrajith, R., Diyabalanage, S., & Dissanayake, C. (2020). Geogenic fluoride and arsenic in groundwater of Sri Lanka and its implications to community health. *Groundwater for Sustainable Development*, 10, 100359.
- Changsheng, H., Akram, W., Rashid, A., Ullah, Z., Shah, M., Alrefaei, A. F., Kamel, M., Aleya, L., & Abdel-Daim, M. M. (2022). Quality assessment of groundwater based on geochemical modelling and water quality index (WQI). *Water*, 14(23), 3888.
- Chaudhari, S., Parmar, H. & Samnani, P. (2024) Human nutritional condition and dental fluorosis in populations with varying concentrations of fluoride in their water sources. In: *Advanced treatment technologies for fluoride removal in water: Water purification*.) Springer, pp. 251–269.
- Chen, J., Qian, H., Wu, H., Gao, Y., & Li, X. (2017). Assessment of arsenic and fluoride pollution in groundwater in Dawukou area, Northwest China, and the associated health risk for inhabitants. *Environmental Earth Sciences*, 76, 1–15.
- Dinç, G., & Güll, A. (2022). Estimation of effective spatial variables when visiting public squares through factor analysis model. *Journal of Urban Planning and Development*, 148(3), 04022022.
- Epa, U. (2001) Risk assessment guidance for superfund: Volume III—part A, Process for conducting probabilistic risk assessment.) US environmental protection agency Washington, DC, USA.
- Farag, M. A., Abib, B., Qin, Z., Ze, X. and Ali, S. E. (2023) Dietary macrominerals: Updated review of their role and orchestration in human nutrition throughout the life cycle with sex differences. *Current Research in Food Science*: 100450.
- Farid, I., Zouari, K., Rigane, A., & Beji, R. (2015). Origin of the groundwater salinity and geochemical processes in detrital and carbonate aquifers: Case of Chougaifiya basin (Central Tunisia). *Journal of Hydrology*, 530, 508–532.
- Fatima, S. U., Khan, M. A., Siddiqui, F., Mahmood, N., Salman, N., Alamgir, A., & Shaukat, S. S. (2022). Geospatial assessment of water quality using principal components analysis (PCA) and water quality index (WQI) in Basho Valley, Gilgit Baltistan (Northern Areas of Pakistan). *Environmental Monitoring and Assessment*, 194(3), 151.
- Feng, F., Jia, Y., Yang, Y., Huan, H., Lian, X., Xu, X., Xia, F., Han, X., & Jiang, Y. (2020). Hydrogeochemical and statistical analysis of high fluoride groundwater in northern China. *Environmental Science and Pollution Research*, 27, 34840–34861.
- Fuge, R. (2019). Fluorine in the environment, a review of its sources and geochemistry. *Applied Geochemistry*, 100, 393–406.
- Ghafat, H., Nazzal, Y., Batayneh, A., Zumlot, T., Zaman, H., Elawadi, E., Laboun, A., Mogren, S., & Qaisi, S. (2014). Geochemical assessment of groundwater contamination with special emphasis on fluoride, a case study from Midyan Basin, northwestern Saudi Arabia. *Environmental Earth Sciences*, 71, 1495–1505.
- Gibbs, G. (1977). A study of the structural chemistry of coesite. *Zeitschrift für Kristallographie-Crystalline Materials*, 145(1–6), 108–123.

- Gibbs, R. J. (1970). Mechanisms controlling world water chemistry. *Science*, 170(3962), 1088–1090.
- Hayat, E., & Baba, A. (2017). Quality of groundwater resources in Afghanistan. *Environmental Monitoring and Assessment*, 189, 1–16.
- Islam, M. S. (2023). Groundwater: Sources, functions, and quality. In *Hydrogeochemical evaluation and groundwater quality*. Springer, pp. 17–36.
- Jamali, M. A., Markhand, A. H., Kumar, D., Arain, A. Y. W., & Mahar, M. H. (2023). The investigation of heavy metal concentration through GIS-based approach from groundwater of Umerkot city, Sindh, Pakistan. *Arabian Journal of Geosciences*, 16(2), 134.
- Jannat, J. N., Khan, M. S. I., Islam, H. T., Islam, M. S., Khan, R., Siddique, M. a. B., Varol, M., Tokatli, C., Pal, S. C. & Islam, A. (2022). Hydro-chemical assessment of fluoride and nitrate in groundwater from east and west coasts of Bangladesh and India. *Journal of Cleaner Production*, 372, 133675.
- Jenckes, J., Muñoz, S., Ibarra, D., Boutt, D., & Munk, L. (2024). Geochemical weathering variability in high latitude watersheds of the Gulf of Alaska. *Journal of Geophysical Research: Earth Surface*, 129(3), e2023JF007284.
- Jha, P. K., & Tripathi, P. (2021). Arsenic and fluoride contamination in groundwater: A review of global scenarios with special reference to India. *Groundwater for Sustainable Development*, 13, 100576.
- Jiang, C., Li, M., Li, C., Huang, W., & Zheng, L. (2023). Combining hydrochemistry and  $^{13}\text{C}$  analysis to reveal the sources and contributions of dissolved inorganic carbon in the groundwater of coal mining areas, in East China. *Environmental Geochemistry and Health*, 45(10), 7065–7080.
- Kar, S. (2022). Geochemical Characteristics of mineral elements: Arsenic, fluorine, lead, nitrogen, and carbon. In *Structure and functions of pedosphere*. Springer, pp. 209–254.
- Khattak, J. A., Farooqi, A., Hussain, I., Kumar, A., Singh, C. K., Mailloux, B. J., Bostick, B., Ellis, T., & Van Geen, A. (2022). Groundwater fluoride across the Punjab plains of Pakistan and India: Distribution and underlying mechanisms. *Science of the Total Environment*, 806, 151353.
- Khattak, S. A., Rashid, A., Tariq, M., Ali, L., Gao, X., Ayub, M., & Javed, A. (2021). Potential risk and source distribution of groundwater contamination by mercury in district Swabi, Pakistan: Application of multivariate study. *Environment, Development and Sustainability*, 23, 2279–2297.
- Kumar, P., Kumar, M., Barnawi, A. B., Maurya, P., Singh, S., Shah, D., Yadav, V. K., Kumar, A., Kumar, R. and Yadav, K. K. (2023) A review on fluoride contamination in groundwater and human health implications and its remediation: A sustainable approaches. *Environmental Toxicology and Pharmacology*: 104356.
- Li, C., Gao, X., Zhang, X., Wang, Y., & Howard, K. (2022). Groundwater fluoride and arsenic mobilization in a typical deep aquifer system within a semi-arid basin. *Journal of Hydrology*, 609, 127767.
- Mcmahon, P. B., Brown, C. J., Johnson, T. D., Belitz, K., & Lindsey, B. D. (2020). Fluoride occurrence in United States groundwater. *Science of the Total Environment*, 732, 139217.
- Mwiathi, N. F., Gao, X., Li, C., & Rashid, A. (2022). The occurrence of geogenic fluoride in shallow aquifers of Kenya Rift Valley and its implications in groundwater management. *Ecotoxicology and Environmental Safety*, 229, 113046.
- Nath, A., Bhuyan, P., Gogoi, N. and Deka, P. (2023) Pesticides and chemical fertilizers: Role in soil degradation, groundwater contamination, and human health. In *Xenobiotics in urban ecosystems: Sources, distribution and health impacts*) Springer, pp. 131–160.
- Nizam, S., Virk, H. S., & Sen, I. S. (2022). High levels of fluoride in groundwater from Northern parts of Indo-Gangetic plains reveals detrimental fluorosis health risks. *Environmental Advances*, 8, 100200.
- Noor, R., Maqsood, A., Baig, A., Pande, C. B., Zahra, S. M., Saad, A., Anwar, M., & Singh, S. K. (2023). A comprehensive review on water pollution, South Asia Region: Pakistan. *Urban Climate*, 48, 101413.
- Noor, S., Rashid, A., Javed, A., Khattak, J. A., & Farooqi, A. (2022). Hydrogeological properties, sources provenance, and health risk exposure of fluoride in the groundwater of Batkhela, Pakistan. *Environmental Technology, Innovation*, 25, 102239.
- Obrike, S., Saleh, A., Iyakwari, S., Anudu, G., & Magaji, I. (2023). Hydro-geochemical evolution, quality, and health risk assessment of groundwater in crystalline basement aquifer in Keffi, Nigeria. *International Journal of Energy and Water Resources*, 1–20.
- Ochoa-Rivero, J. M., Jacquez-Herrera, V., Prieto-Amparán, J. A., Loya-Fierro, O., Ballinas-Casarrubias, L., González-Horta, C., Olmos-Marquez, M. A., & Rocha-Gutiérrez, B. A. (2023) Risk assessment for the distribution and levels of fluoride and nitrate in groundwater in a semi-arid area of northern Mexico. *Groundwater for Sustainable Development*, 101045.
- Parrone, D., Ghergo, S., Frollini, E., Rossi, D., & Preziosi, E. (2020). Arsenic-fluoride co-contamination in groundwater: Background and anomalies in a volcanic-sedimentary aquifer in central Italy. *Journal of Geochemical Exploration*, 217, 106590.
- Prema & Patil, S. (2022) Hydro-geo chemical analysis of groundwater and surface water near Bhima River Basin Jewargi Taluka Kalburgi, Karnataka. In *Recent trends in construction technology and management: Select proceedings of ACTM 2021*) Springer, pp. 361–372.
- Rafiq, M., & Jan, M. Q. (1989). Geochemistry and petrogenesis of Ambela granitic complex, NW Pakistan. *Geological Bulletin, University of Peshawar*, 22, 159–179.
- Rahman, M. M., Bodrud-Doza, M., Siddiqua, M. T., Zahid, A., & Islam, A. R. M. T. (2020). Spatiotemporal distribution of fluoride in drinking water and associated probabilistic human health risk appraisal in the coastal region, Bangladesh. *Science of the Total Environment*, 724, 138316.
- Rashid, A., Ayub, M., Bundschuh, J., Gao, X., Ullah, Z., Ali, L., Li, C., Ahmad, A., Khan, S. and Rinklebe, J. (2023a) Geochemical control, water quality indexing, source distribution, and potential health risk of fluoride and arsenic in groundwater: Occurrence, sources apportionment, and positive matrix factorization model. *Journal of Hazardous Materials*, 460, 132443. <https://doi.org/10.1016/j.jhazmat.2023.132443>

- Rashid, A., Ayub, M., Bundschuh, J., Gao, X., Ullah, Z., Ali, L., Li, C., Ahmad, A., Khan, S., & Rinklebe, J. (2023). Geochemical control, water quality indexing, source distribution, and potential health risk of fluoride and arsenic in groundwater: Occurrence, sources apportionment, and positive matrix factorization model. *Journal of Hazardous Materials*, 460, 132443.
- Rashid, A., Ayub, M., Bundschuh, J., Gao, X., Ullah, Z., Ali, L., Li, C., Ahmad, A., Khan, S., Rinklebe, J., & Ahmad, P. (2023c). Geochemical control, water quality indexing, source distribution, and potential health risk of fluoride and arsenic in groundwater: Occurrence, sources apportionment, and positive matrix factorization model. *Journal of Hazardous Materials*, 132443.
- Rashid, A., Ayub, M., Gao, X., Khattak, S. A., Ali, L., Li, C., Ahmad, A., Khan, S., Rinklebe, J., & Ahmad, P. (2024). Hydrogeochemical characteristics, stable isotopes, positive matrix factorization, source apportionment, and health risk of high fluoride groundwater in semiarid region. *Journal of Hazardous Materials*, 469, 134023.
- Rashid, A., Ayub, M., Gao, X., Xu, Y., Ullah, Z., Zhu, Y. G., Ali, L., Li, C., Ahmad, A., & Rinklebe, J. (2024). Unraveling the impact of high arsenic, fluoride and microbial population in community tubewell water around coal mines in a semiarid region: Insight from health hazards, and geographic information systems. *Journal of Hazardous Materials*, 480, 136064.
- Rashid, A., Ayub, M., Javed, A., Khan, S., Gao, X., Li, C., Ullah, Z., Sardar, T., Muhammad, J., & Nazneen, S. (2021). Potentially harmful metals, and health risk evaluation in groundwater of Mardan, Pakistan: Application of geostatistical approach and geographic information system. *Geoscience Frontiers*, 12(3), 101128.
- Rashid, A., Ayub, M., Khan, S., Ullah, Z., Ali, L., Gao, X., Li, C., El-Serehy, H. A., Kaushik, P., & Rasool, A. (2022). Hydrogeochemical assessment of carcinogenic and non-carcinogenic health risks of potentially toxic elements in aquifers of the Hindukush ranges, Pakistan: Insights from groundwater pollution indexing, GIS-based, and multivariate statistical approaches. *Environmental Science and Pollution Research*, 29(50), 75744–75768.
- Rashid, A., Ayub, M., Ullah, Z., Ali, A., Khattak, S. A., Ali, L., Gao, X., Li, C., Khan, S., & El-Serehy, H. A. (2022). Geochemical modeling source provenance, public health exposure, and evaluating potentially harmful elements in groundwater: Statistical and human health risk assessment (HHRA). *International Journal of Environmental Research and Public Health*, 19(11), 6472.
- Rashid, A., Ayub, M., Ullah, Z., Ali, A., Sardar, T., Iqbal, J., Gao, X., Bundschuh, J., Li, C., & Khattak, S. A. (2023). Groundwater quality, health risk assessment, and source distribution of heavy metals contamination around chromite mines: Application of GIS, sustainable groundwater management, geostatistics, PCAMLR, and PMF receptor model. *International Journal of Environmental Research and Public Health*, 20(3), 2113.
- Rashid, A., Farooqi, A., Gao, X., Zahir, S., Noor, S., & Khattak, J. A. (2020). Geochemical modeling, source apportionment, health risk exposure and control of higher fluoride in groundwater of sub-district Dargai, Pakistan. *Chemosphere*, 243, 125409.
- Rashid, A., Guan, D.-X., Farooqi, A., Khan, S., Zahir, S., Jehan, S., Khattak, S. A., Khan, M. S., & Khan, R. (2018). Fluoride prevalence in groundwater around a fluorite mining area in the flood plain of the River Swat, Pakistan. *Science of the Total Environment*, 635, 203–215.
- Rashid, A., Khan, S., Ayub, M., Sardar, T., Jehan, S., Zahir, S., Khan, M. S., Muhammad, J., Khan, R., & Ali, A. (2019). Mapping human health risk from exposure to potential toxic metal contamination in groundwater of Lower Dir, Pakistan: Application of multivariate and geographical information system. *Chemosphere*, 225, 785–795.
- Rehman, F., Siddique, J., Shahab, A., Azeem, T., Bangash, A. A., Naseem, A. A., Riaz, O., & Ur Rehman, Q. (2022). Hydrochemical appraisal of fluoride contamination in groundwater and human health risk assessment at Isa Khel, Punjab, Pakistan. *Environmental Technology, Innovation*, 27, 102445.
- Saeed, T. U., Aziz, A., Khan, T. A., & Attaullah, H. (2012). Application of geographical information system (GIS) to groundwater quality investigation: A case study of Mardan district, Pakistan. *International Journal of Physical Sciences*, 7(37), 5421–5448.
- Sarkar, S., Mukherjee, A., Chakraborty, M., Quamar, M. T., Duttagupta, S., & Bhattacharya, A. (2023). Prediction of elevated groundwater fluoride across India using multi-model approach: Insights on the influence of geologic and environmental factors. *Environmental Science and Pollution Research*, 30(11), 31998–32013.
- Sathe, S. S., Mahanta, C., & Subbiah, S. (2021). Hydrogeochemical evaluation of intermittent alluvial aquifers controlling arsenic and fluoride contamination and corresponding health risk assessment. *Exposure and Health*, 13(4), 661–680.
- Shah, M. T., & Danishwar, S. (2003). Potential fluoride contamination in the drinking water of Naranji area, northwest frontier province, Pakistan. *Environmental Geochemistry and Health*, 25(4), 475–481.
- Shaji, E., Sarath, K., Santosh, M., Krishnaprasad, P., Arya, B., & Babu, M. S. (2024). Fluoride contamination in groundwater: A global review of the status, processes, challenges, and remedial measures. *Geoscience Frontiers*, 15(2), 101734.
- Singh, L. P., & Kshetrimayum, K. (2021). Evaluation of spatial characteristics of groundwater hydrochemical constituents across different geomorphic units of the Imphal Valley in Northeast India. *Sustainable Water Resources Management*, 7, 1–18.
- Su, H., Kang, W., Li, Y., & Li, Z. (2021). Fluoride and nitrate contamination of groundwater in the Loess Plateau, China: Sources and related human health risks. *Environmental Pollution*, 286, 117287.
- Talpur, S. A., Noonari, T. M., Rashid, A., Ahmed, A., Jat Baloch, M. Y., Talpur, H. A., & Soomro, M. H. (2020). Hydrogeochemical signatures and suitability assessment of groundwater with elevated fluoride in unconfined aquifers Badin district, Sindh, Pakistan. *SN Applied Sciences*, 2, 1–15.
- Tanui, F., Olago, D., Dulo, S., Ouma, G., & Kuria, Z. (2020). Hydrogeochemistry of a strategic alluvial aquifer system

- in a semi-arid setting and its implications for potable urban water supply: The Lodwar Alluvial Aquifer System (LAAS). *Groundwater for Sustainable Development*, 11, 100451.
- Tiwari, K., Krishan, G., Prasad, G., Mondal, N., & Bhardwaj, V. (2020). Evaluation of fluoride contamination in groundwater in a semi-arid region, Dausa District, Rajasthan, India. *Groundwater for Sustainable Development*, 11, 100465.
- Tokath, C., Onur, S. G., Dindar, M. B., Malafaia, G., Islam, A. R. M. T., & Muhammad, S. (2023). Spatial-temporal variability and probabilistic health risk assessment of fluoride from lentic ecosystem, Türkiye. *International Journal of Environmental Analytical Chemistry*, 1–20.
- Ullah, Z., Rashid, A., Ghani, J., Nawab, J., Zeng, X.-C., Shah, M., Alrefaei, A. F., Kamel, M., Aleya, L., & Abdel-Daim, M. M. (2022). Groundwater contamination through potentially harmful metals and its implications in groundwater management. *Frontiers in Environmental Science*, 10, 1021596.
- Ullah, Z., Rashid, A., Nawab, J., Bacha, A.-U.-R., Ghani, J., Iqbal, J., Zhu, Z., Alrefaei, A. F., & Almutairi, M. H. (2023). Fluoride contamination in groundwater of community tube wells, source distribution, associated health risk exposure, and suitability analysis for drinking from arid zone. *Water*, 15(21), 3740.
- Ullah, Z., Xu, Y., Zeng, X.-C., Rashid, A., Ali, A., Iqbal, J., Almutairi, M. H., Aleya, L., Abdel-Daim, M. M., & Shah, M. (2022). Non-carcinogenic health risk evaluation of elevated fluoride in groundwater and its suitability assessment for drinking purposes based on water quality index. *International Journal of Environmental Research and Public Health*, 19(15), 9071.
- Varol, S., & Davraz, A. (2014). Assessment of geochemistry and hydrogeochemical processes in groundwater of the Tefenni plain (Burdur/Turkey). *Environmental Earth Sciences*, 71, 4657–4673.
- Wallick, E. (1981). Chemical evolution of groundwater in a drainage basin of Holocene age, east-central Alberta, Canada. *Journal of Hydrology*, 54(1–3), 245–283.
- Wang, Z., Zhang, Z., Adimalla, N., Guo, H., Pei, J., & Liu, H. (2024). Spatial distribution and enrichment mechanisms of high fluoride groundwater in geotherm-affected Pliocene aquifers of the Guide basin, China. *Journal of Geochemical Exploration*, 256, 107356.
- Who, G. (2011). Guidelines for drinking-water quality. *World Health Organization*, 216, 303–304.
- Xaza, A. (2020) *Investigating hydrogeochemical processes of groundwater*. Heuningnes Catchment.
- Xie, X., Shi, J., Pi, K., Deng, Y., Yan, B., Tong, L., Yao, L., Dong, Y., Li, J., & Ma, L. (2023). Groundwater quality and public health. *Annual Review of Environment and Resources*, 48(1), 395–418.
- Yeşilnacar, M. İ., Demir Yetiş, A., Dülgergil, Ç. T., Kumral, M., Atasoy, A. D., Rastgeldi Doğan, T., Tekiner, S. İ., Bayhan, I., & Aydoğdu, M. (2016). Geomedical assessment of an area having high-fluoride groundwater in southeastern Turkey. *Environmental Earth Sciences*, 75, 1–14.
- Young, S. M., Pitawala, A., & Ishiga, H. (2011). Factors controlling fluoride contents of groundwater in north-central and northwestern Sri Lanka. *Environmental Earth Sciences*, 63, 1333–1342.

**Publisher's Note** Springer Nature remains neutral with regard to jurisdictional claims in published maps and institutional affiliations.

Springer Nature or its licensor (e.g. a society or other partner) holds exclusive rights to this article under a publishing agreement with the author(s) or other rightholder(s); author self-archiving of the accepted manuscript version of this article is solely governed by the terms of such publishing agreement and applicable law.